

Design and analysis of an optimal hopper for use in resonance-based locomotion

Ivor Wanders

Robotics and Mechatronics group
CTIT institute

University of Twente

`i.wanders@alumnus.utwente.nl`

Gerrit A. Folkertsma

Robotics and Mechatronics group
CTIT institute

University of Twente

`g.a.folkertsma@ieee.org`

Stefano Stramigioli

Robotics and Mechatronics group
CTIT institute

University of Twente

`s.stramigioli@ieee.org`

Abstract—**Quadrupedal running is an efficient form of locomotion found in nature, which serves as an inspiration for robotics. We believe that a resonance-based approach is the path towards energy-efficient legged locomotion and running robots. The first step in working towards this goal is creating an energy-efficient one-legged hopper. Such a one-legged hopper was designed and constructed. The impact efficiency of the mechanism is calculated analytically, determined in simulation and measured with the prototype. The impact efficiency as calculated from the experiments is found to be in agreement with the analytical expectation and simulation results. Finally, using an electric motor to inject energy by creating a virtual spring with reverse hysteresis, hopping is achieved with the prototype.**

I. INTRODUCTION

Quadrupedal running consists of coordinated periodic motions that, in nature, form a fast and energy-efficient bound or gallop. This form of locomotion has been an inspiration for the field of robotics for years. However, we have still not achieved the graceful, fast movement; nor matched this energy-efficiency in quadrupedal robots. We believe one of the steps towards this goal is to exploit the periodicity of the locomotion, by using resonance to generate the motions and improve energy-efficiency: just like in nature [1].

Animals have a certain degree of elasticity in their tendons and muscles [2]. As such, the stiffness is also incorporated in models of walking, for example in the SLIP model [3], [4]. The compliance in legs is useful to absorb shocks from impact, as in MIT’s cheetah, in which elastic tendons introduce compliance in the leg mechanism [5], [6]. Another option to introduce compliance is to actuate stiff members in a compliant way, for example with pneumatics as in HyQ [7]. The stiffness of animal legs has been related to their movement speed [8]. This has led other researchers to investigate the application of variable stiffness actuators and mechanisms for use in legged locomotion [9], [10].

To take the concept of compliance in legs further, it would be beneficial to the energy-efficiency if this compliance could be used to facilitate the periodic motion required to move forward. In the field of morphological computation, research is ongoing towards exploiting the body dynamics in achieving desired behaviour [11]. For example, special controllers that make use of the passive dynamics of a system are investigated [12]–[14]. Others use actuators that introduce high-frequency

oscillation and try to find mechanisms that then effectuate forward motion [15]. In spite of all this effort, we have yet to reach the high energy-efficient performance that is seen in nature.

Our goal is to create a robot that can run efficiently and with grace, like a real cheetah does. We intend to use a flexible spine that, combined with front and rear legs, creates the periodic motion seen in animals. Previous research has shown that a spinal joint with a spring can improve the overall energy-efficiency of the robot [6]. Others have shown that a spine with nonlinear stiffness leads to even higher efficiency [16]. In our robot, the front and rear body will be made to bounce on their legs, while the flexible spine introduces a resonance that results in forward motion. For maximally energy-efficient actuation, the front and rear ‘hoppers’ will be actuated in resonance with a controlled offset in their phase, as in [17]. A crucial part of such a resonance-based robot is thus an energy-efficient bouncing leg, i.e. the ‘hopper’.

This paper is about the design and analysis of such a one-legged hopper. The energy loss is investigated in both a mathematical framework and in practice. The design considerations of the mechanism are discussed and the used prototype is described; then the analytical energy loss is determined, as well as the steps necessary to measure the energy loss in practice. Finally, the measurements are shown to be in accordance with the expectations.

II. DESIGN

A. Design Considerations

Our goal for the robot is to have a natural bounding gait, ideally with a leg step frequency of about 1 Hz so that the movement is clearly visible. During the hopping, energy will be lost due to friction and impact on the ground. This energy loss needs to be compensated to sustain continuous hopping. The stance phase is the only period during which energy can be introduced into the system. To allow enough energy to be introduced, we aim for a long stance phase of 50% of the step period.

Assuming the air phase is parabolic, a flight time of half a second implies an initial vertical velocity of $v_0 = gt/2 = 2.45$ m/s. With this vertical velocity, a height of about 30 cm would be reached, regardless of the system’s mass. A small bench top prototype is desired for testing, so a jump height

of 30 cm is considered unpractical. To lower the height, an increase of the stepping frequency is required.

The designed one-legged hopper will be a planar mechanism. This means it can be light, so that the required power and forces in the mechanism are as low as possible. To keep the number of joints (and thereby the amount of friction) low, a parallelogram construction is chosen. This ensures that the leg stays perpendicular to the ground, resulting in a well-defined ground contact point. A spring placed in the diagonal of the parallelogram allows energy storage during compression of the leg. To be able to compensate for the friction and impact losses, a DC motor can be attached to one of the joints with minimal impact on the mechanism's behaviour.

A backdrivable parallel elastics configuration is obtained, so no holding torque is required to be able to store energy in the spring and, therefore, it also allows the leg to function without the motor.

B. System

The prototype is lasercut from DELRIN™ (Polyoxymethylene). The low friction coefficient of this material allows efficient plain bearings to be created by inserting metal rods through smooth drillholes. The thickness for all structural members is 6 mm, the driving axle is a $\varnothing 6$ mm brass cylinder and the other joints are made with $\varnothing 3$ mm polished steel cylinders.

The prototype is attached to a 33 cm long aluminium L-profile (20x20x2 mm), which pivots at the other end to allow upwards motion of the mechanism while constraining the other degrees of freedom. A small DELRIN™ cylinder with a diameter of 2.5 mm is used to reduce the ground contact area and minimise friction.

A relatively low transmission ratio of 1 : 2 is chosen between motor and leg, to allow backdrivability while increasing the torque that can be applied to the rotating elements. The motor used is a Maxon RE-Max 226806, which has a stall torque of 299 mNm [18]. The sensor, an AMS AS5045 rotary position sensor, is mounted collocated to the motor [19].

A schematic drawing of the mechanism is shown in Figure 1 and a photograph of the actual prototype can be seen in Figure 2. Relevant parameter values of the mechanism are listed in Table I. The rotating elements are present in an upper pair and lower pair, but in the table their mass is combined as M_1 .

III. METHOD

A. Analytical

To obtain an analytical description of the system, the Lagrangian equations are used to derive the generalized robotics equation:

$$\mathbf{M}(\mathbf{q})\ddot{\mathbf{q}} + \mathbf{C}(\mathbf{q}, \dot{\mathbf{q}})\dot{\mathbf{q}} + \mathbf{N}(\mathbf{q}, \dot{\mathbf{q}}) = \mathbf{F}. \quad (1)$$

For the analytical derivation of the impact loss, the mechanism is reduced to the one depicted in Figure 3. This

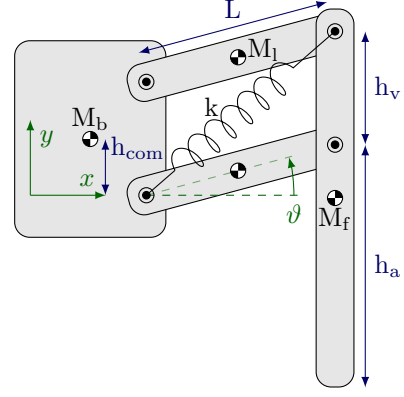


Fig. 1. Schematic diagram of the one-legged hopper. The three degrees of freedom are x and y for the translation of the body and the angle ϑ of the leg. The relevant parameters are listed in Table I.

TABLE I
PROPERTIES OF THE MECHANISM.

Symbol	Value with motor (without)	Unit
M_b	370 (210)	gram
M_1	28.0	gram
M_f	11.5	gram
L	8.0	centimeter
h_v	6.0	centimeter
h_a	7.4	centimeter
k	368.6 (184.3)	newton/meter

results in the following terms for \mathbf{M} , \mathbf{C} and \mathbf{N} :

$$\mathbf{M}(\mathbf{q}) = \begin{bmatrix} (M_b + M_L) & 0 & -\sin(q_3)\gamma \\ 0 & (M_b + M_L) & \cos(q_3)\gamma \\ -\sin(q_3)\gamma & \cos(q_3)\gamma & L^2(\frac{1}{4}M_1 + M_f) + I_{leg} \end{bmatrix},$$

$$\mathbf{C}(\mathbf{q}, \dot{\mathbf{q}})\dot{\mathbf{q}} = \begin{bmatrix} -\dot{q}_3^2 \cos(q_3)\gamma \\ -\dot{q}_3^2 \sin(q_3)\gamma \\ -\dot{q}_1 \dot{q}_3 \cos(q_3)\gamma - \dot{q}_2 \dot{q}_3 \sin(q_3)\gamma \end{bmatrix},$$

$$\mathbf{N}(\mathbf{q}, \dot{\mathbf{q}}) = \begin{bmatrix} 0 \\ g(M_b + M_L) \\ g \cos(q_3)\gamma \end{bmatrix}, \quad \mathbf{F} = \begin{bmatrix} F_x \\ F_y \\ \tau \end{bmatrix},$$

where $\gamma = L(\frac{1}{2}M_1 + M_f)$, $I_{leg} = \frac{1}{12}M_1L^2$ and $M_L = M_1 + M_f$.

This description of the system can subsequently be used to determine the theoretical impact efficiency. To this end, the Pfaffian constraints of the system at ground contact are identified. When the system is in contact with the ground, it can be described by:

$$\mathbf{M}(\mathbf{q})\ddot{\mathbf{q}} + \mathbf{C}(\mathbf{q}, \dot{\mathbf{q}})\dot{\mathbf{q}} + \mathbf{N}(\mathbf{q}, \dot{\mathbf{q}}) = \mathbf{F} + \mathbf{A}(\mathbf{q})\lambda, \quad (2)$$

$$\mathbf{A}^\top(\mathbf{q})\dot{\mathbf{q}} = 0.$$

When contact is made with the ground, the foot (x_f, y_f) does not move any more. The constraint equation for the system is then given by:

$$\mathbf{A}^\top(\mathbf{q})\dot{\mathbf{q}} = \begin{bmatrix} 1 & 0 & -L \sin(q_3) \\ 0 & 1 & L \cos(q_3) \end{bmatrix} \begin{bmatrix} \dot{q}_1 \\ \dot{q}_2 \\ \dot{q}_3 \end{bmatrix} = \begin{bmatrix} \dot{x}_f \\ \dot{y}_f \end{bmatrix} = \begin{bmatrix} 0 \\ 0 \end{bmatrix}. \quad (3)$$

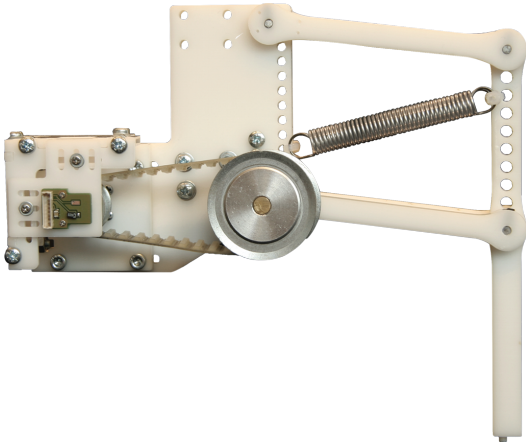


Fig. 2. Photograph of the mechanism with the motor mount attached. The green PCB holds the rotary position sensor. The motor is mounted behind the main body element, coaxially to the sensor.

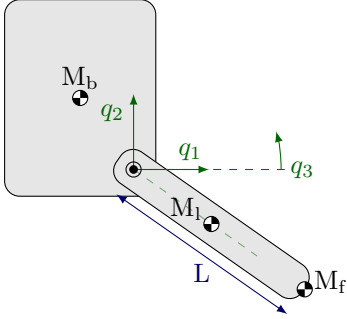


Fig. 3. Reduced mechanism for the analytical consideration. The degrees of freedom q_1 and q_2 correspond to the translation of the body x and y in Figure 1, q_3 corresponds to the leg angle ϑ . The relevant parameters are listed in Table I.

The instantaneous impact is considered: let t^- be the time just before the impact and t^+ the time after the impact. Equation (2) can be integrated over time, under the assumption that $\mathbf{q}(t^+) \approx \mathbf{q}(t^-)$, because $t^+ \approx t^-$. This results in:

$$\mathbf{M}(\mathbf{q})\dot{\mathbf{q}}(t^+) - \mathbf{M}(\mathbf{q})\dot{\mathbf{q}}(t^-) = \mathbf{A}(\mathbf{q}) \int_{t^-}^{t^+} \lambda(t) dt, \quad (4)$$

$$\mathbf{A}^\top(\mathbf{q})\dot{\mathbf{q}}(t^+) = 0. \quad (5)$$

Left multiplying (4) by $\mathbf{M}^{-1}(\mathbf{q})$, subsequent left multiplication by $\mathbf{A}^\top(\mathbf{q})$ and substitution with (5) results in (\mathbf{q} as argument left out for clarity):

$$- (\mathbf{A}^\top \mathbf{M}^{-1} \mathbf{A})^{-1} \mathbf{A}^\top \dot{\mathbf{q}}(t^-) = \int_{t^-}^{t^+} \lambda(t) dt. \quad (6)$$

Substituting (6) back into (4) allows the expression to be written without the integral:

$$\mathbf{M}\dot{\mathbf{q}}(t^+) - \mathbf{M}\dot{\mathbf{q}}(t^-) = -\mathbf{A} (\mathbf{A}^\top \mathbf{M}^{-1} \mathbf{A})^{-1} \mathbf{A}^\top \dot{\mathbf{q}}(t^-), \quad (7)$$

$$\dot{\mathbf{q}}(t^+) = (\mathbf{I} - \mathbf{M}^{-1} \mathbf{A} (\mathbf{A}^\top \mathbf{M}^{-1} \mathbf{A})^{-1} \mathbf{A}^\top) \dot{\mathbf{q}}(t^-). \quad (8)$$

This result is an explicit equation that relates the velocity $\dot{\mathbf{q}}$ after the impact to the velocity before the impact. By combining this relation with the expression for the kinetic co-energy before and after the impact, a relation for energy loss due to impact is found:

$$\Delta E_k = \frac{1}{2} \dot{\mathbf{q}}(t^+)^\top \mathbf{M} \dot{\mathbf{q}}(t^+) - \frac{1}{2} \dot{\mathbf{q}}(t^-)^\top \mathbf{M} \dot{\mathbf{q}}(t^-) \quad (9)$$

$$= -\frac{1}{2} \dot{\mathbf{q}}(t^-)^\top (\mathbf{A} (\mathbf{A}^\top \mathbf{M}^{-1} \mathbf{A})^{-1} \mathbf{A}^\top) \dot{\mathbf{q}}(t^-). \quad (10)$$

The impact efficiency η is expressed as the ratio of energy after impact to energy before impact:

$$\eta = \frac{E_k^+}{E_k^-} = \frac{E_k^- + \Delta E_k}{E_k^-}. \quad (11)$$

B. Simulation

The mechanism described in II-B is modelled as four rigid bodies connected by rotational joints. These are simulated in the modelling and simulation package 20SIM [20]. The properties of the elements are made identical to the values from the prototype.

The ground contact is modelled as a combination of a Hunt-Crossley model [21] for normal force (12) and Coulomb friction (13).

$$F_y = K_c \cdot \delta + K_d \cdot |\delta| \cdot \dot{\delta}. \quad (12)$$

$$F_x = -\mu \cdot F_y \cdot \text{sgn}(v_x). \quad (13)$$

This ground contact is tuned such that a deflection δ of the foot is less than 1 mm into the ground and the ground contact is critically damped. A linear guide is simulated by constraining all degrees of freedom but the vertical translation; this guide is attached to either the foot or the body element. The impact efficiency calculation is trivial, as the energy in the system is known.

C. Real World

The prototype, as described in subsection II-B, can also be used to determine the impact efficiency in the real world. For these measurements, the motor was removed and a spring with a lower stiffness was used. Furthermore, a piece of nylon string was attached between the other corners of the parallelogram to configure the impact angle.

The energy loss during the impact cannot be measured directly, but needs to be calculated from other—measurable—values: only the angle ϑ can be measured. In the following energy calculations, all mass except the body mass is considered negligible.

When the mechanism is dropped from a predetermined height (h_{df} , measured from the foot down), the energy before impact is known. Just before impact, at $t = t^-$, the total energy E^- consists of the kinetic energy from the drop, the potential energy from the remaining height and the energy stored in the spring (E_u):

$$\begin{aligned} E^- &= E_p + E_k^- + E_u \\ &= (h_a - L \sin(\vartheta^-) + h_{com}) M_b g + h_{df} M_b g + E_u(\vartheta^-). \end{aligned} \quad (14)$$

Immediately after impact, at $t = t^+$, the only term that is changed (and therefore unknown) is the kinetic energy E_k^+ . An instantaneous change is considered, so the angle is unchanged ($\vartheta^+ \approx \vartheta^-$):

$$\begin{aligned} E^+ &= E_p + E_k^+ + E_u \\ &= (h_a - L \sin(\vartheta^+) + h_{\text{com}}) M_b g + E_k^+ + E_u(\vartheta^+). \end{aligned} \quad (15)$$

After the impact, the leg continues to compress, up to the point of maximum compression at $t = t^*$. At this point the kinetic energy is zero.

$$\begin{aligned} E^* &= E_p + 0 + E_u \\ &= (h_a - L \sin(\vartheta^*) + h_{\text{com}}) M_b g + 0 + E_u(\vartheta^*). \end{aligned} \quad (16)$$

The energy terms (16) and (14) can be subtracted from each other which, combined with $\vartheta^+ \approx \vartheta^-$, results in:

$$\begin{aligned} E^+ - E^* &= (-L \sin(\vartheta^-) + L \sin(\vartheta^*)) M_b g \\ &\quad + E_k^+ + E_u(\vartheta^-) - E_u(\vartheta^*). \end{aligned} \quad (17)$$

The assumption is made that there is no energy lost during the compression of the leg from after the impact up to the point of maximum compression:

$$E^+ \approx E^* \quad (18)$$

With this assumption, expression (17) is equal to zero, which means the term E_k^+ can be expressed as:

$$\begin{aligned} E_k^+ &= -(-L \sin(\vartheta^-) + L \sin(\vartheta^*)) M_b g \\ &\quad - (E_u(\vartheta^-) - E_u(\vartheta^*)). \end{aligned} \quad (19)$$

This shows that the kinetic energy in the system before the impact and after the impact can be determined by only measuring the leg angle ϑ . The impact efficiency can again be calculated with (11).

IV. RESULTS

A. Impact

To obtain values of the impact efficiency in the real world, the prototype was dropped as described in subsection III-C. Over 500 experiments were carried out with varying impact angles, logging the angle ϑ at 100 Hz.

The measured angle profiles of all these measurements are shown in Figure 4. Test runs with equal impact angles show almost identical angle profiles, even though the setup was moved and measurements were performed over a two-day timespan. This shows that the repeatability is very high.

The impact efficiency for each test run is graphed in Figure 5(a). The analytical impact efficiency, as determined with (11) and (10), is also plotted. Additionally, a least squares fit was made through the points. The function fitted is:

$$\eta_{\text{fit}}(\vartheta) = v_0 (A \cos(2\vartheta) - B). \quad (20)$$

This function is obtained after all the parameters are substituted into the analytical equation for impact efficiency. The terms A and B are dependent on the masses and lengths in the mechanism. This fit is made because the dynamics of the pivoting boom are not considered in the analytical derivation.

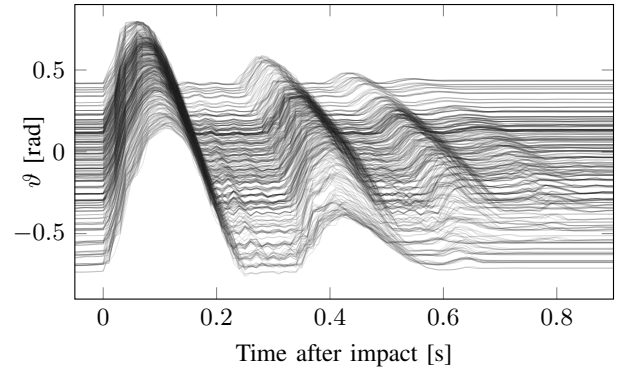


Fig. 4. Plot of ϑ for all impact measurement tests. Every measurement is represented by one semi-transparent line. The highest peak, roughly around $t = 0.1$ s corresponds to t^* : the point of maximum leg compression. The subsequent peaks are from bounces on the floor.

With slightly changed parameters, this fit aligns well with the measurements. However, the measurements seem to be somewhat skewed compared to the analytical fit.

To investigate the cause of this skew, the dynamic model of subsection III-B was used to replicate these experiments in simulation. In the theoretical consideration, the leg is unable to slip. However, in the prototype, the body is constrained in rotation but the leg slides over the floor during the compression phase. As such, simulations were performed with both the linear guide attached to the leg element and the guide attached to the body element. The obtained impact efficiencies are graphed in Figure 5(b).

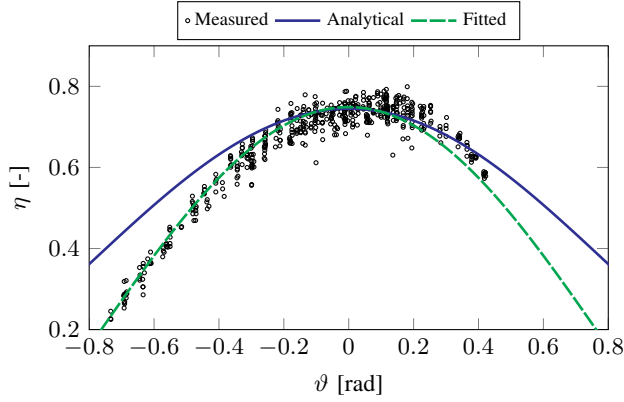
When the linear guide is attached to the foot element, the assumption that no energy is lost during compression (18) is correct. However, when the linear guide is attached to the body element, the foot is able to slide over the floor, resulting in energy loss due to friction. This results in the skewed line seen in Figure 5(b). Surprisingly, the simulated impact efficiencies were higher than expected from the theory. This can be attributed to the visco-elastic ground contact model, which results in less energy loss than the instantaneous impact used in the analytical description.

B. Hopping

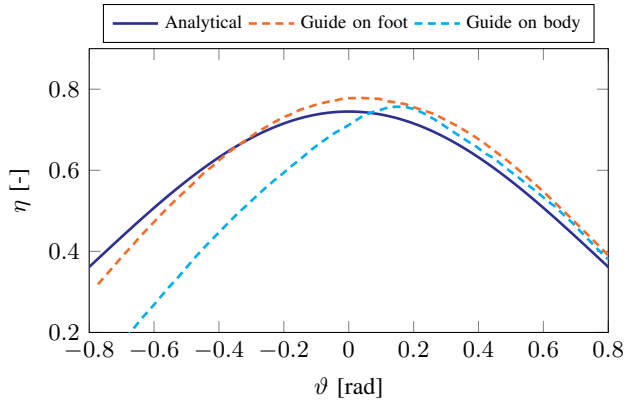
The goal of the research is to obtain a hopping leg. Therefore, the prototype was also used to attempt this hopping. The purpose of the motor and controller is to inject energy into the system to compensate for friction and impact losses.

Our approach is to use the motor to create a virtual spring with negative hysteresis, similar to [22]: we create the hysteresis not by switching the equilibrium position of the spring, but by changing the virtual spring's stiffness, as illustrated in Figure 6. The energy injected is the area enclosed by the curve and is thus directly dependent on the amount of hysteresis. The virtual spring allows us to change the effective leg stiffness and thus change the resonance frequency.

The measurements of the hopping are shown in Figure 7. The frequency of hopping is around 2 Hz, so only slightly higher than our original goal of 1 Hz. The hopping achieved



(a) Calculated impact efficiencies from the analytical model, as measured and a fit through the points.



(b) Impact efficiency as found with simulation, compared with analytical results. Simulations performed with the linear guide attached to either the body element or the foot element.

Fig. 5. Impact efficiency calculations, measurements and simulation results. The impact efficiency is defined as $\eta = E_k^+ / E_k^-$.

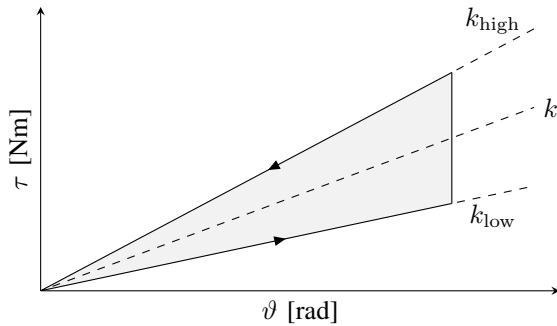


Fig. 6. Diagram of the virtual spring created inside the controller. If the leg starts compressing at $\vartheta = 0$, the stiffness is low (k_{low}) up to the point of maximum compression. At this point the controller increases the virtual spring stiffness to k_{high} and the leg starts extending back to the origin.

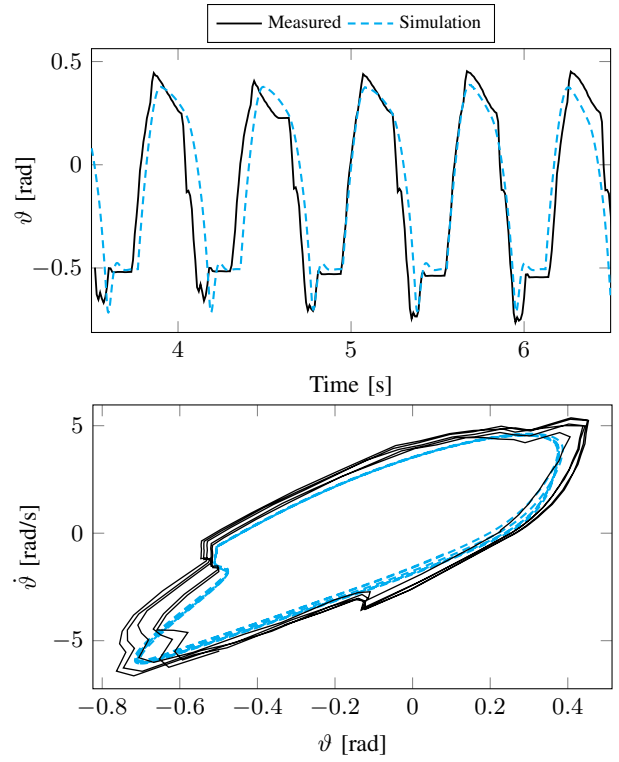


Fig. 7. Comparison between the simulated hopping and measurements of the hopping prototype. At the top: leg angle ϑ against time, at the bottom the phaseplot of ϑ . The mechanism is clear of the ground around $\vartheta = -0.5$, where the leg reaches its maximum extension before the motor is used to hold the leg at $\vartheta = -0.5$.

in the simulation is also graphed; these results are in close agreement with the measurements.

The hysteresis required for hopping was very large and the stiffness during the compression phase was even negative. An adverse effect of the large hysteresis, combined with the low transmission ratio, is that the motor almost continuously has to deliver maximum torque. This quickly heats up the motor, which means sustained hopping is not possible.

Why this large hysteresis is required is not immediately apparent. The impact efficiency is obviously very good, as seen in Figure 5(a). There is some friction in the joints, but it is very low: Figure 4 shows the hopper completely clears the ground once or twice, without any energy injection. This can only mean that the problem is in the drive-chain: the low transmission ratio results in a very high motor torque, thereby operating the motor in a very inefficient region. Increasing the transmission ratio would increase the efficiency of the motor, but is detrimental to the backdrivability of the mechanism and results in higher impact losses. Instead, we propose a new design where the drive-chain includes a series elastics element, allowing a high transmission ratio while retaining backdrivability. Figure 8 illustrates the concept.

V. CONCLUSION

We have designed and constructed a simple and affordable leg mechanism for resonance-based locomotion. A mathematical description of this mechanism was derived, ultimately

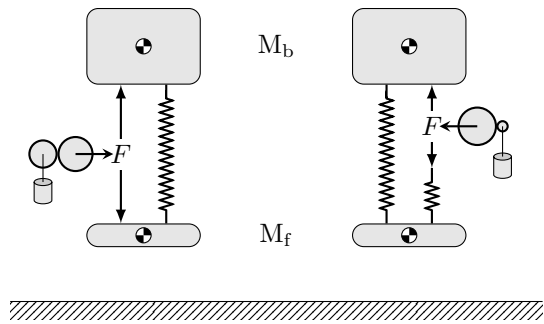


Fig. 8. Left: the current prototype. With a relatively low transmission to allow backdrivability the motor has to rotate slowly and is far from its optimal operating speed. Right: proposed new design with series elastics. A higher transmission is possible, resulting in higher motor speeds and the backdrivability is maintained by the spring in series with the transmission.

leading to an expression for the theoretical impact efficiency. The proposed mechanism was built and used to compare this analytical expression to the real world. The measured results were found to correspond well with the theoretical expectations.

The mechanism was also shown to be capable of hopping. However, the low motor speed and consequently high torque requirements result in the motor heating up. This problem cannot be fixed by increasing the transmission ratio, as this affects the backdrivability of the drive-chain. We intend to solve this problem with a combination of a series elastics drive-chain and parallel stiffness.

With this work, we have gained more insight into the impact loss of mechanisms for legged locomotion. Currently we are developing an improved prototype for use in a combination of such hoppers, which will be used in experiments that aim to realise graceful, resonance-based locomotion.

REFERENCES

- [1] B. K. Ahlborn and R. W. Blake, "Walking and running at resonance," *Zoology (Jena)*, vol. 105, no. 2, pp. 165–174, 2002.
- [2] R. Alexander and H. Bennet-Clark, "Storage of elastic strain energy in muscle and other tissues," *Nature*, vol. 265, no. 5590, pp. 114–117, 1977.
- [3] R. J. Full and D. E. Koditschek, "Templates and anchors: neuromechanical hypotheses of legged locomotion on land," *J. Exp. Biol.*, vol. 202, no. Pt 23, pp. 3325–3332, Dec 1999.
- [4] R. M. Ghigliazza, R. Altendorfer, P. Holmes, and D. Koditschek, "A simply stabilized running model," *SIAM Rev.*, vol. 47, no. 3, pp. 519–549, Mar. 2005. [Online]. Available: <http://dx.doi.org/10.1137/050626594>
- [5] S. Seok, A. Wang, M. Y. Chuah, D. Otten, J. Lang, and S. Kim, "Design principles for highly efficient quadrupeds and implementation on the mit cheetah robot," in *Robotics and Automation (ICRA), 2013 IEEE International Conference on*, May 2013, pp. 3307–3312.
- [6] G. A. Folkertsma, S. Kim, and S. Stramigioli, "Parallel stiffness in a bounding quadruped with flexible spine," in *Intelligent Robots and Systems (IROS), 2012 IEEE/RSJ International Conference on*, Oct 2012, pp. 2210–2215.
- [7] C. Semini, N. G. Tsagarakis, E. Guglielmino, M. Focchi, F. Cannella, and D. G. Caldwell, "Design of hyq - a hydraulically and electrically actuated quadruped robot," *Proceedings of the Institution of Mechanical Engineers, Part I: Journal of Systems and Control Engineering*, 2011. [Online]. Available: <http://pii.sagepub.com/content/early/2011/07/29/0959651811402275.abstract>
- [8] T. A. McMahon and G. C. Cheng, "The mechanics of running: How does stiffness couple with speed?" *Journal of Biomechanics*, vol. 23, Supplement 1, no. 0, pp. 65 – 78, 1990, international Society of Biomechanics. [Online]. Available: <http://www.sciencedirect.com/science/article/pii/0021929090900422>
- [9] J. Hurst, J. Chestnutt, and A. Rizzi, "An actuator with physically variable stiffness for highly dynamic legged locomotion," in *Robotics and Automation, 2004. Proceedings. ICRA '04. 2004 IEEE International Conference on*, vol. 5, April 2004, pp. 4662–4667 Vol.5.
- [10] H. Vu, H. Hauser, D. Leach, and R. Pfeifer, "A variable stiffness mechanism for improving energy efficiency of a planar single-legged hopping robot," in *Advanced Robotics (ICAR), 2013 16th International Conference on*, Nov 2013, pp. 1–7.
- [11] R. Pfeifer and G. Gómez, "Morphological computation - connecting brain, body, and environment," in *Creating Brain-Like Intelligence*, ser. Lecture Notes in Computer Science, B. Sendhoff, E. Körner, O. Sporns, H. Ritter, and K. Doya, Eds. Springer Berlin Heidelberg, 2009, vol. 5436, pp. 66–83. [Online]. Available: http://dx.doi.org/10.1007/978-3-642-00616-6_5
- [12] M. Uemura and S. Kawamura, "Resonance-based motion control method for multi-joint robot through combining stiffness adaptation and iterative learning control," in *Robotics and Automation, 2009. ICRA '09. IEEE International Conference on*, May 2009, pp. 1543–1548.
- [13] J. Buchli, F. Iida, and A. J. Ijspeert, "Finding resonance: Adaptive frequency oscillators for dynamic legged locomotion," in *In Proceedings iros 2006*. (In. Springer Verlag, 2006, pp. 3903–3909.
- [14] F. Iida, G. Gomez, and R. Pfeifer, "Exploiting body dynamics for controlling a running quadruped robot," in *Advanced Robotics, 2005. ICAR '05. Proceedings., 12th International Conference on*, July 2005, pp. 229–235.
- [15] N. Maheshwari, X. Yu, M. Reis, and F. Iida, "Resonance based multi-gaited robot locomotion," in *Intelligent Robots and Systems (IROS), 2012 IEEE/RSJ International Conference on*, Oct 2012, pp. 169–174.
- [16] M. Khoramshahi, H. J. Bidgoly, S. Shafiee, A. Asaei, A. J. Ijspeert, and M. N. Ahmadbadi, "Piecewise linear spine for speed - energy efficiency trade-off in quadruped robots," *Robotics and Autonomous Systems*, vol. 61, no. 12, pp. 1350 – 1359, 2013. [Online]. Available: <http://www.sciencedirect.com/science/article/pii/S0921889013001425>
- [17] G. A. Folkertsma, S. Stramigioli, and A. J. van der Schaft, "Power-continuous synchronisation of oscillators: a novel, energy-free way to synchronise dynamical systems," in *Proceedings of the 2014 IEEE International Conference on Robotics & Automation (ICRA 2014), Hong Kong, China*. USA: IEEE Robotics and Automation Society, June 2014.
- [18] M. M. Ag., "Re-max 29 ø29 mm, graphite brushes, 22 watt, with terminals," September 2014. [Online]. Available: <http://www.maxonmotor.com/maxon/view/product/226806>
- [19] A. ag., "As5045 - 12 bit rotary position sensor - ams," September 2014. [Online]. Available: <http://www.ams.com/eng/Products/Position-Sensors/Magnetic-Rotary-Position-Sensors/AS5045>
- [20] C. P. B.V., "20sim," September 2014. [Online]. Available: <http://www.20sim.com/>
- [21] K. H. Hunt and F. R. E. Crossley, "Coefficient of restitution interpreted as damping in vibroimpact," *Journal of Applied Mechanics*, vol. 42, no. 2, pp. 440–445, 1975. [Online]. Available: <http://dx.doi.org/10.1115/1.3423596>
- [22] D. Lakatos, M. Görner, F. Petit, A. Dietrich, and A. Albu-Schäffer, "A modally adaptive control for multi-contact cyclic motions in compliantly actuated robotic systems," in *International Conference on Intelligent Robots and Systems*, ser. Proceedings of IEEE/RSJ International Conference on Intelligent Robots and Systems, November 2013, pp. 5388–5395. [Online]. Available: <http://elib.dlr.de/85549/>